Residue 19 of the Parathyroid Hormone: Structural Consequences†

Andrea Piserchio,‡ Naoto Shimizu,§ Thomas J. Gardella,§ and Dale F. Mierke*,‡,||

Department of Chemistry and Department of Molecular Pharmacology, Division of Biology & Medicine, Brown University, Providence, Rhode Island 02912, and Endocrine Unit, Massachusetts General Hospital and Harvard Medical School, Boston, Massachusetts 02114

Received May 21, 2002; Revised Manuscript Received July 16, 2002

ABSTRACT: Residue 19 of the parathyroid hormone (PTH) has been shown to play an important role in both binding to and activation of the PTH receptor; specifically, Arg^{19}-containing analogues have improved biological function over similar Glu^{19} peptides {Shimizu et al. (2002) *Biochemistry 41*, 13224−13233}. Additionally the juxtamembrane portion of the receptor is involved in the different biological responses. Here, we determine the conformational preferences of PTH analogues to provide a structural basis for their biological actions. On the basis of circular dichroism results, the $Arg^{19} \rightarrow Glu^{19}$ mutations within the context of both PTH(1−20) and PTH(1−34) analogues lead to increases in helix content, ranging from a 8−15% increase. High-resolution structures as determined by ^{1}H NMR and NOE-restrained molecular dynamics simulations clearly illustrate the difference between Arg^{19} and Glu^{19}−PTH(1−20), particularly with the extent and stability of the C-terminal helix. The Arg^{19}-containing analogue has a well defined, stable α-helix from Ser^4−Arg^{19}, while the Glu^{19} analogue is less ordered at the C-terminus. On the basis of these observations, we propose that position 19 of PTH(1−20) must be α-helical for optimal interaction with the juxtamembrane portion of the receptor. This mode of binding extends the current view of PTH binding (indeed ligand binding for all class B GPCRs), which invokes a bihelical ligand with the C-terminus of the ligand interacting with the N-terminus of the receptor (responsible for binding) and the N-terminus of the ligand interacting with the seven-helical bundle (leading to receptor activation).

Parathyroid hormone (PTH)[1] as the major regulator of serum calcium levels has been intensely studied as a possible therapy for osteoporosis. Through modifications of the N-terminal 34 amino acids of PTH, it has been clearly demonstrated that the C-terminus of PTH(1−34) plays a major role in binding to the G-protein coupled receptor for PTH (PTH1); the N-terminus of PTH(1−34) is required for receptor activation. Most recent efforts in the development of structure−activity relationships have therefore targeted one of these domains, further probing their distinct roles in the biological action of PTH. Much less effort has been carried out in defining the role of the region of PTH linking the N-terminus (activation domain) and C-terminus (binding domain). In the accompanying manuscript (*1*), we describe the pharmacological characterization of a series of analogues probing the role of residue 19 of PTH, both in PTH(1−34) and N-terminal truncated PTH(1−20) analogues.

Here, we detail the structural features of these PTH analogues as determined by circular dichroism (CD), high-resolution nuclear magnetic resonance (NMR), and extensive computer simulations. The investigation was carried out in a membrane-like milieu in order to mimic the environment in which the ligand interacts with the receptor. A comparison of these results, coupled with the pharmacological characterization of the analogues at the wild-type PTH1 receptor and modified PTH1 receptors presented in the accompanying manuscript (*1*), allows for clarification of the functional role of residue 19 in the biological actions of PTH.

EXPERIMENTAL PROCEDURES

Peptides. The peptides used in this study were prepared using Fmoc-based, solid-phase synthesis as described in the accompanying manuscript (*1*). The sequences of the analogues examined and related peptides are given in Table 1.

Circular Dichroism. Circular dichroism spectra were recorded on a Jasco model 710 spectropolarimeter; peptides were analyzed at a concentration of 20 μM in 50 mM sodium phosphate buffer pH 7.4 containing 2,2,2-trifluoroethanol at 20% (v/v). Spectroscopic scans were performed at 20 °C and at wavelengths between 185 and 255 nm, with data recorded at each 1 nm interval. Eight scans were accumulated and averaged for each sample. At each wavelength, the mean

† This work was supported in part by the National Institute of Health through Grants DK-11794 (T.J.G.) and GM-54082 (D.F.M.).

* Corresponding author. Address: Department of Molecular Pharmacology, Division of Biology & Medicine, Brown University, Providence RI, 02912. Phone: (401) 863-2139. Fax: (401) 863-1595. E-mail: Dale_Mierke@Brown.edu.

‡ Department of Chemistry, Brown University.

§ Massachusetts General Hospital and Harvard Medical School.

|| Department of Molecular Pharmacology, Brown University.

[1] Abbreviations: CD, circular dichroism; DG, distance geometry; DPC, dodecylphosphocholine; G Protein, guanine nucleotide-binding regulatory protein; Har, homoarginine; MD, molecular dynamics; NMR, nuclear magnetic resonance; NOE, nuclear Overhauser enhancement; NOESY, nuclear Overhauser enhancement spectroscopy; PACAP, pituitary adenylyl cyclase-activating peptide; PTH, parathyroid hormone; PTH1, parathyroid hormone receptor 1; PTHrP, parathyroid hormone related protein; RMSD, root-mean-square-deviation; TOCSY, total-correlation spectroscopy.

10.1021/bi0261600 CCC: $22.00
Published on Web 10/08/2002

Table 1: Amino Acid Sequences and Nomenclature of the PTH Analogs Examined Here[a]

PTH(1−20)	S-V-S-E-I-Q-L-M-H-N-L -G-K-H-L-N-S-M-E-R
[M]PTH(1−20)	A-V-A-E-I-Q-L-M-H-Q-Har-A-K-W-L-N-S-M-R-R
[M]PTH(1−20)−Glu^{19}	A-V-A-E-I-Q-L-M-H-Q-Har-A-K-W-L-N-S-M-E-R

[a] M = Ala^{1,3,12},Gln^{10},Har^{11},Trp^{14},Arg^{19}. Har = homoarginine.

residue molar elipticity [θ] (in dimensions of deg cM dmol^{-1}) was calculated by the equation: $[\theta] = \theta * 100/l * C * n$; where θ is the raw ellipticity value (in dimensions of millidegree), l is the sample path length in centimeters, C is the molar peptide concentration, and n is the number of residues in the peptide (*2*). The helical content of each peptide was estimated by dividing [θ] observed at 222 nm for that peptide by −33 100 (*2*, *3*).

NMR Methods. Solutions approximately 1 mM were prepared by dissolving the solid samples in 600 μL of a 50 mM phosphate buffer solution (5% D_2O, pH 6.5 uncorrected for isotope affect) containing 150 mM NaCl and 180 mM dodecylphosphocholine-d_{38} (DPC, Cambridge Isotopes Laboratories).

The NMR spectra were collected at 600 MHz on a Bruker Avance instrument at 298 and 308 K. All the amino acids spin systems were identified by running TOCSY (*4*) experiments with mixing times ranging between 20 and 65 ms, all implementing the MLEV-17 pulse sequence (*5*) for the Harman−Hahn transfer. For the sequential assignment and the structural analysis of the peptides, NOESY experiments (*6*) with mixing times of 150 ms were employed. The WATERGATE sequence was used in all the experiments to achieve water suppression (*7*). The ^{1}H chemical shifts were referenced respect to the signal of perdeuterated 3-(trimethylsilyl) propionate sodium salt (TSP, 0.0 ppm).

All the spectra were processed using the NMRPipe software (*8*). The indirect dimension was expanded to 1024 points using a linear prediction algorithm. Prior to Fourier transformation, Gaussian and shifted squared sine bell apodization functions were applied in the directly detected and in the incremented dimension, respectively. The program Sparky (*9*) was used to assign and to integrate the peaks of the processed NMR spectra. The resulting volumes were converted into interproton distances applying the two spin approximation and using a set of calibration peaks generated by geminal β and γ protons, indole protons, and well-resolved helical αH−NH interactions. The secondary shifts for Hα protons were calculated by subtracting the chemical shift values for random coil from the measured resonances and averaging over three residues (*10*). During this procedure homoarginine (Har) was treated as an arginine.

Distance Geometry. A matrix of experimental upper and lower bounds was obtained by adding and subtracting 15% to the NOE-derived distances and applying a pseudoatom corrections to the upper bounds of methyl groups and of the unresolved methylene protons (*11*). This matrix was then merged with a second matrix representing the molecular constitution of the polypeptide (holonomic matrix). From the resulting distance matrix 100 molecular structures were generated in four dimensions using the random metrization algorithm (*12*). The structures were then optimized by conjugate gradients and by a simplified simulated annealing protocol initially in four, and finally in three dimensions. The resulting structures showing NOE violations greater than 0.3 Å or structural distortions were discarded. All the calculations were performed on Pentium III processors using home written programs.

MD Simulations. A representative DG structure was energy minimized in vacuo with conjugate gradients in the AMBER force field (disregarding charges) using DISCOVER (Molecular Simulations, Inc.). Using the GROMACS program (*13*), the molecule was then soaked into a periodic cubic two phases box ($5.5 \times 5.0 \times 5.0$ nm^3) containing typically around 2100 molecules of water and 130 molecules of decane. The peptide was oriented at the water−decane interface using Insight II (Molecular Simulations, Inc.). All the atoms from the peptide were treated explicitly in the GROMOS-87 force field including Lennard-Jones (1 nm cutoff), Coulomb (1 nm cutoff), and standard bonded (bond-stretching, angle bending, improper, and proper dihedrals) potential functions. A description of the water−decane interface appeared elsewhere (*14*). The charges of the ionizable groups were defined accordingly to the experimental pH, no counterions were added. The system was energy minimized, and the solvent−peptide interactions were optimized running a 10 ps MD at 300 K constraining the positions of the peptide atoms.

The experimental distance restraints were then introduced with a force constant of 2000 kJ mol^{-1} nm^{-1}. The final molecular dynamics simulations were run for 600 ps using GROMACS (*13*). An integration time step of 2 fs, a constant pressure of 1 bar (independent in all the three dimensions, coupling constant of 0.2 ps), and a constant temperature of 300K (independent coupling for decane, water, and peptide, coupling constant of 0.02 ps) were applied. Simulations were carried out on three Pentium III processors. Analysis of the results was performed using the GROMACS package.

RESULTS

CD Spectroscopy. As an initial screen for structural differences associated with modification of position 19, CD spectra were collected and compared for a series of PTH peptides, including PTH(1−34), [M]PTH(1−34), PTH(1−20), and [M]PTH(1−20). In Figure 1 we compare the CD spectra for pairs of PTH peptides wherein the two peptides of each pair differ only by having Arg or Glu at position 19, (indicated by solid and dotted lines, respectively, in Figure 1A−D). As shown in Figure 1, all of the peptides, measured in a 50 mM phosphate solution containing 20% 2,2,2-trifluorethanol (TFE), contained some helical structure, as indicated by the positive deflection in the spectra at ∼190 nm and the negative deflections at ∼208 and 222 nm. In comparing the paired spectra, the CD bands were consistently stronger for the Arg^{19}-containing peptide than they were for the corresponding Glu^{19}-containing analogue; the helical content (calculated from the mean residue ellipticity observed at 222 nM, $[\theta]_{222}$) of each of these Arg^{19}-containing analogues was 8 to 15% higher than that of the corresponding Glu^{19}-containing analogue. Specifically, the difference between [M]PTH(1−20) and [M]PTH(1−20)−Glu^{19} is the largest (15%) with helix content values of 78% and 63%, respectively (assuming a maximum mean residue ellipticity of −33 000 for an α-helix) (*3*).

NMR Spectroscopy. The Hα secondary shifts of [M]PTH-(1−20) indicate that a large percentage of the peptide is

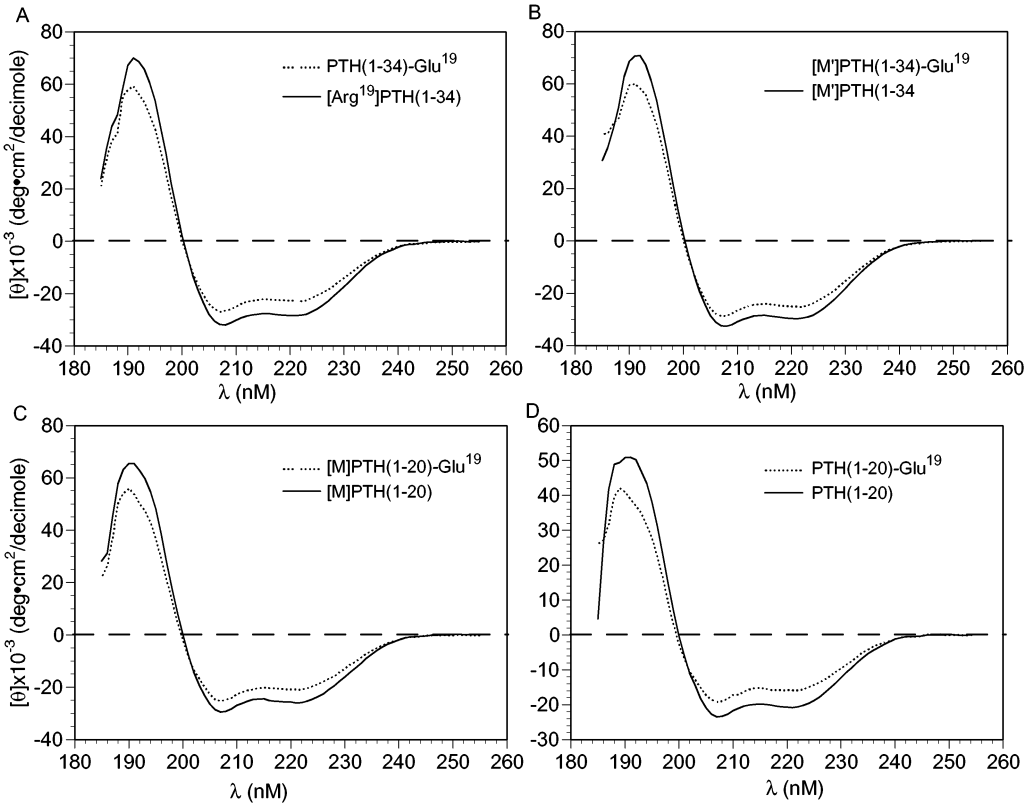

FIGURE 1: Effect of the $Glu^{19} \rightarrow Arg$ substitution on secondary structure of several PTH analogues was analyzed by CD spectroscopy. Spectra were recorded at a peptide concentration of 20 μM, in 50 mM sodium phosphate buffer, pH 7.4 containing 2,2,2-trifluoroethanol (20% v/v), as described in Materials and Methods.

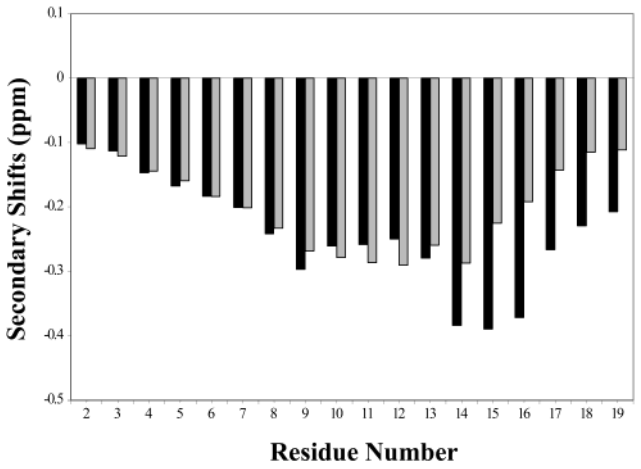

FIGURE 2: Hα secondary shifts for [M]PTH(1−20) (black bars) and [M]PTH(1−20)−Glu^{19} (gray bars). The chemical shifts were measured relative to TSP collected at 35 °C.

helical (Figure 2). This is more evident for the central portion of the molecule (residues His^9−Asn^{16}), but the C-terminus also exhibits strong negative deviation with respect to random coil values. The helical content seems to decrease while moving toward the N-terminus where the secondary shifts of the first three residues are close to the random coil values.

The observed pattern of NOEs is in accord with the secondary shifts (Figure 3). All of the sequential NH(i)−NH(i+1) interactions between resolved peaks are observed starting from residue Ala^3. The canonical helical NOEs (i.e., Hα(i)−HN(i+3,4) and Hα(i)−Hβ(i+3)) were detected starting from residue Glu^4. Additionally, a medium range NOE (Val^2 Hα−Ile^5 Hβ) was observed in the N-terminus (Figure 4). A total of 161 NOE derived distance constraints (38 medium range, 50 sequential) were utilized in the DG-based structural refinement, with 78 structures fulfilling the experimental restraints accepted for further analysis.

The results from the analysis of the conformational space sampled by the DG program indicates a well-defined α-helical motif encompassing residues Gln^{10}−Arg^{20}. Between residue Ile^5 and His^9, a helical shape is predominant but less tightly defined (Figure 5). It should be noticed that many NH and Hα resonances in this area are overlapped and some of the possible helical NOEs could not be confirmed (the secondary shifts, clearly indicating helix, are not used as restraints during the DG calculations). Finally, the backbone conformation of the N-terminus is poorly ordered and on average mainly extended.

After the first 300 ps of MD simulation, all the residues included in the fragment Glu^4−Arg^{19} have converged toward an α-helix, including the residues between Glu^4 and His^9 whose dihedral angles diverged from the canonical α-helical values in the starting structure. The adoption of more standard α-helices mainly comes from the hydrogen bonding between i,i+4 residues; the DG calculations do not account for the partial charges of the amide and carbonyl groups. During the MD simulations, the first three residues undergo several transitions among mainly extended conformations. The peptide tends to orient the helical hydrophobic face, which includes residues Ile^5, Leu^7, Met^8, Trp^{14}, Leu^{15}, and Met^{18} toward the decane surface (Figure 6). On the opposite face of the helix the charged residues Har^{11}, Lys^{13}, and Arg^{20}, and the hydrophilic residues Gln^6 and Gln^{10} project their side-chains toward the water phase.

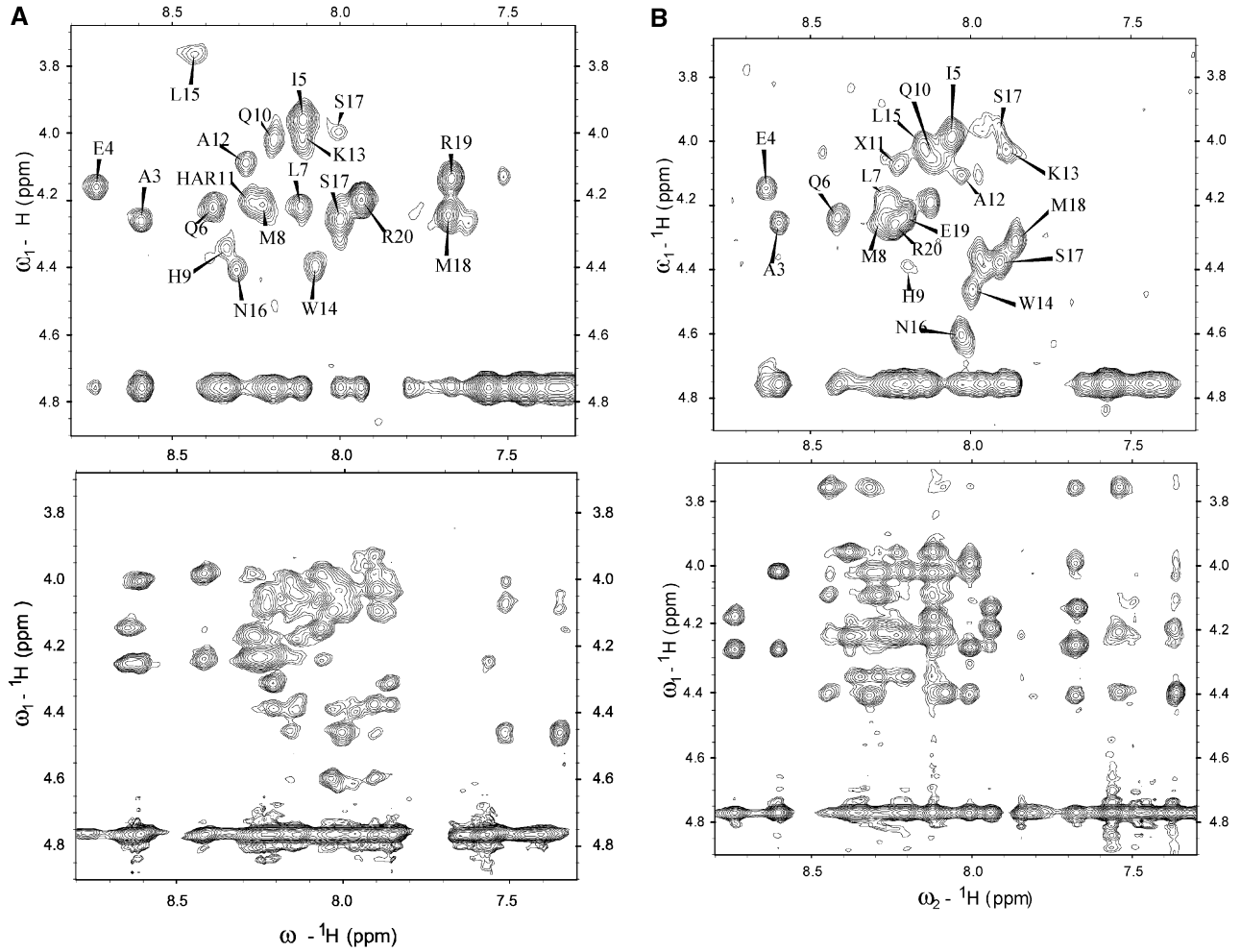

FIGURE 3: Expanded portion of exemplary TOCSY (top) and NOESY (bottom) spectra for [M]PTH(1−20) (A) and [M]PTH(1−20)−Glu^{19} (B). The assignments of the amide protons are denoted in the TOCSY spectra.

[M]PTH(1−20)−Glu^{19}. The Hα secondary shifts of the Glu^{19}-containing analogue is illustrated in Figure 2. In the N-terminus, residues Ala^1−Trp^{14}, the shifts are similar to those observed for the Arg^{19}-containing analogue. Starting from Leu^{15} on toward the C-terminus, the secondary shifts are diminished by approximately 50% when compared to those of [M]PTH(1−20) (Figure 2). These results (suggesting that 30% of the peptide is 50% less helical) are in general agreement with the data from CD.

Similar to [M]PTH(1−20), all of the NH(i)−NH(i+1) NOEs between resolved amides are observed. The NOEs characterizing α-helices are widely detected in the region between residues Ile^5 and Leu^{15}. Many medium range NOEs identified in the previous analogue between Ser^{17} and Arg^{20} are either absent or of very low intensity. Similarly to [M]-PTH(1−20), few medium range distance restraints have been identified in the N-terminus, suggesting conformational heterogeneity for the N-terminal 3 residues. A total of 140 NOEs (30 medium range, 42 sequential) were utilized in the DG calculations, with a total of 72 DG structures accepted for further refinement. Analyzing the ϕ,ψ distribution of the resulting DG structures indicates a strong preference for Glu^4−Ser^{17} for helical conformations (Figure 5).

During the first 300 ps of MD simulations, the roughly helical structure obtained from DG adopts a well defined α-helix between residues Glu^4 and Ser^{17} which is maintained during the simulation. Again the two termini are flexible and fail to adopt a stable, long-lived conformation. The amphipathic helix of the peptide orients itself at the two phase interface similarly to that observed for [M]PTH(1−20) (Figure 7).

DISCUSSION

In the accompanying manuscript, we have illustrated that residue 19, changing the charge from negative to positive (Glu^{19} → Arg^{19}), has a dramatic effect on the binding to (ca. 100 fold increase) and activation of (ca. 10-fold increase) the wild-type PTH1 receptor when incorporated into the N-terminal [M]PTH(1−20) analogue (*1*). Here, we place these biological findings onto a structural framework. Using spectroscopic techniques we probe for structural changes that may account for the observed pharmacological results.

Circular dichroism provides a facile method for characterization of overall, major structural changes, particularly in the content of secondary structural elements, induced by modification of residue 19. These studies were carried out in the presence of 20% TFE, a well-established solvent for the study of the propensity of the peptide (or protein) toward helical formation. The results of these experiments indicated that the Arg^{19} substitution (relative to the native Glu^{19}) increased helicity in each of the peptides examined (Figure 1). Therefore, there is a correlation between helicity of these analogues and their capacity to interact productively with

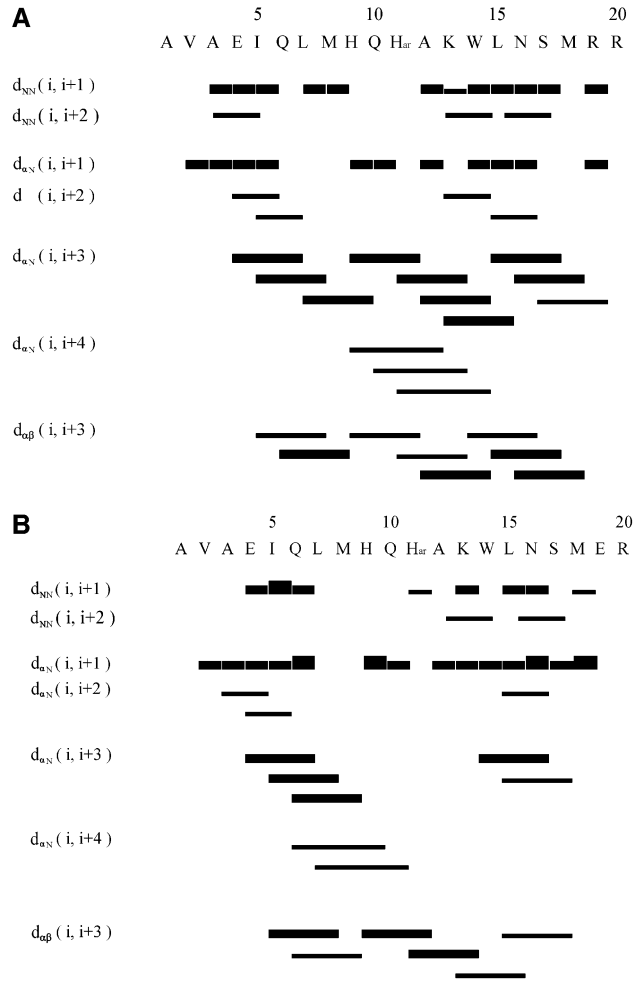

FIGURE 4: Summary of the NOEs observed for [M]PTH(1−20) (A) and [M]PTH(1−20)−Glu[19] (B).

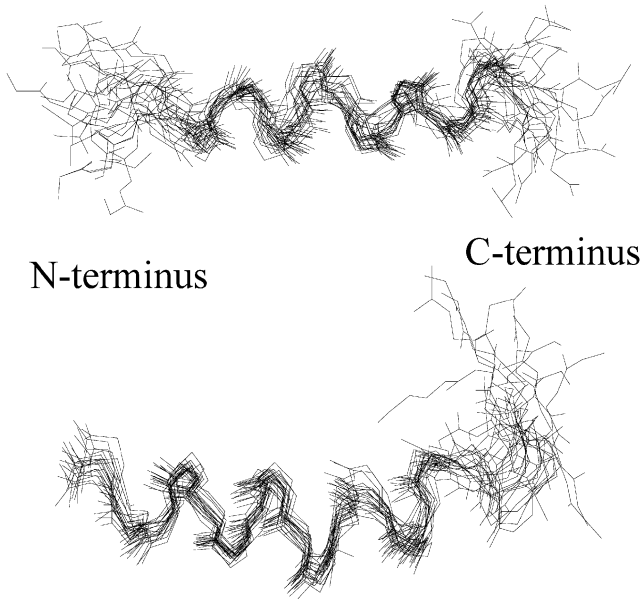

FIGURE 5: Superposition of 20 structures with the lowest penalty from the DG calculations, [M]PTH(1−20) (top; RMSD 0.9 Å for residues E^4−R^{20}) and [M]PTH(1−20)−Glu^{19} (bottom; RMSD 1.7 Å for residues E^4−S^{17}).

the PTH1 receptor. Of course, the CD analysis only provides the content of secondary structure, not the specific location of these elements. To address this point, high-resolution

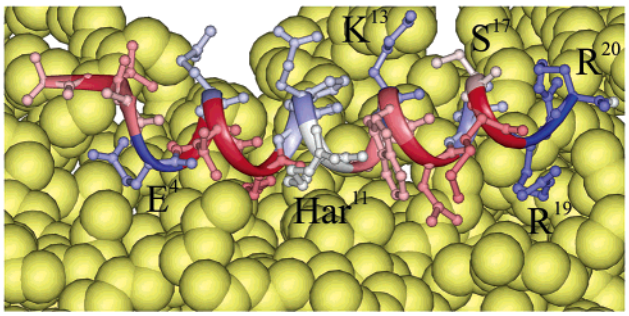

FIGURE 6: Structure of [M]PTH(1−20) following an NOE-restrained MD simulation for 300 ps in a water−decane membrane mimetic solvent box with periodic boundary conditions. The amino acids of the receptor fragment are color coded according to hydrophobicity (blue = polar, red = hydrophobic), with the N- and C-termini depicted on the left and right, respectively. The decane phase is depicted in gold CPK, and the water phase has been omitted for clarity.

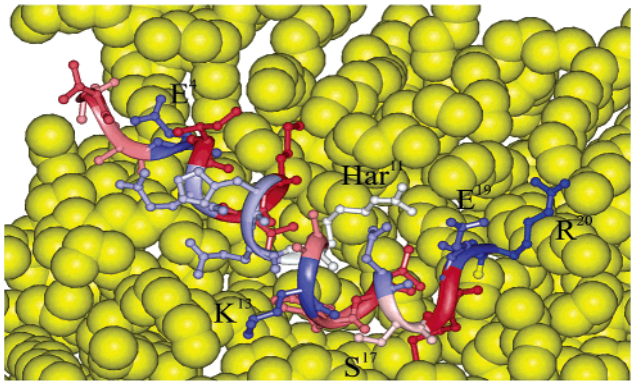

FIGURE 7: Structure of [M]PTH(1−20)−Glu^{19} following NOE-restrained MD simulations (see Figure 6 caption for details).

NMR studies were carried out on [M]PTH(1−20) and [M]-PTH(1−20)−Glu^{19}.

The NMR studies of [M]PTH(1−20) and [M]PTH(1−20)−Glu^{19} were carried out in the presence of micelles of dodecylphosphocholine. The rapid and isotropic reorientation of the lipid micelles provides a zwitterionic membrane mimetic that is amenable to NMR based structural studies in solution. Studying the peptide in such an environment is important, given the accumulating evidence that the ligand−receptor interaction is mediated through a membrane associated pathway, originally put fourth by Schwyzer based on ligand targeting the neurokinin-1 receptor (*15*−*17*) and further examined by ligands tethered to the membrane by Moroder (*18*, *19*). Indeed, studies of the pituitary adenylyl cyclase-activating peptide (PACAP) while bound to DPC micelles and to its receptor (closely related to the PTH1 receptor) illustrated only minor differences (*20*). These results are completely consistent with preabsorption of the ligand to the membrane followed by the interaction between the preorganized ligand and receptor.

The structural features as determined by NMR and extensive structure refinement indicate a large content of α-helix for both [M]PTH(1−20) and [M]PTH(1−20)−Glu^{19}; indeed, through the refined structures from the NOE-restrained MD simulations, we observe 80% and 70% helicity for the Arg^{19} and Glu^{19} analogues, respectively. These results are similar to the helical contents measured by CD in the presence of TFE (i.e., 78 and 63%, respectively). The major

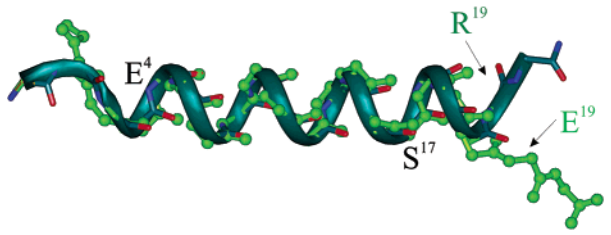

FIGURE 8: Superposition of residues 4−17 of the structures of [M]-PTH(1−20) (dark green ribbon, side chains illustrated) and [M]-PTH(1−20)−Glu[19] (light green ribbon) following NOE-restrained MD simulations.

structural differences between [M]PTH(1−20) and [M]PTH-(1−20)−Glu[19] resides in the C-terminus; [M]PTH(1−20) is almost completely α-helix, while the C-terminus of [M]PTH-(1−20)−Glu[19] is structurally disordered beyond Ser[17], as illustrated in Figure 8. These conclusions are consistent with all of the NMR observables, including secondary shift of the Hα protons (Figure 2) and NOEs (Figure 4). The incorporation of the positively charged residue, Arg[19], has a dramatic, local effect on the stability of the α-helix. No specific interactions within the peptide can account for this enhanced stability; the residues *i*,*i*+3 and *i*,*i*+4 removed from position 19 (Asn[16] and Leu[15], respectively) would not be expected to display particular affinity or distinction between Glu[19] and Arg[19]. One possibility for the enhanced helicity of Arg[19] is the stabilization of the macrodipole of the α-helix: the positively charged Arg[19] would reinforce the negative dipole found at the C-terminus of helices (Glu[19] would destabilize the α-helix) (*21*). Interestingly, the helix enhancement induced by Arg[19] is also observed within the PTH(1−34) analogues (see Figure 1A,B). Given that position 19 is at the N-terminus of the second α-helix in PTH(1−34) (*22*), the interaction with the macrodipole of the helix cannot account for the helix enhancement in PTH(1−34). Another possibility is that Glu[19] destabilizes the helicity of the C-terminus of PTH(1−20). During the MD simulations of [M]PTH(1−20)−Glu[19], interactions between the side chains of Glu[19] and Har[11] and Arg[20] take place (the former interaction between Har[11]−Glu[19] partially accounts for the folding over of the C-terminus of [M]PTH(1−20)−Glu[19], Figure 8).

There have been a number of studies of analogues of PTH-(1−34) in various solvents by both CD (*23*−*27*) and NMR methods (*22*, *25*, *28*−*31*). The NMR data have typically indicated a short N-terminal helix (ca. residues 3−11), a longer C-terminal helix (ca. residues 17−30), and an intervening turn or flexible hinge region. The importance of this flexible region has been stressed in a number of publications on PTH and the related hormone, parathyroid hormone related protein (PTHrP) (*25*, *32*). Within PTHrP-(1−34), modification of position 19 (Arg[19] → Glu[19]) did not significantly alter the helix content (*32*). On the basis of trNOE results with the related peptide−hormone system PACAP (*20*), a bihelical structure is prevalent when the hormone is bound to the receptor.

In contrast, the present data indicate enhanced biological activity with extending the N-terminal helix up to position 19, which, given that this is the beginning of the C-terminal helix of PTH(1−34) (*22*), suggests that the optimal binding motif may be one extended α-helix. Interestingly, the recent X-ray crystallographic structure of PTH(1−34) reveals a continuous helix that extends nearly the entire length of the molecule (e.g., from residue 3 to 33) (*33*). Indeed, using lactam bridges designed to stabilize α-helices between Lys[13]−Asp[17], Lys[18]−Asp[22], and Lys[26]−Asp[30], Condon and co-workers have produced a potent agonist for the PTH1 receptor (*26*). This would suggest that if there is flexibility between two separate helical regions of the receptor bound PTH(1−34), it would be C-terminal of residue 22. Taken together, these findings serve to highlight the uncertainty in our current view of the bioactive conformation (or conformations) of PTH (*22*,*34*).

The in vitro data of the accompanying manuscript show that the [M]PTH(1−20) containing Arg[19] is one of the most potent N-terminal PTH1 receptor agonist analogues described to date. Importantly, the enhanced binding and potency of the Arg[19] analogues is maintained when the large N-terminus of the PTH1 receptor is removed; the peptide with the extended N-terminal helix is 12 times more active in stimulating cAMP accumulation than the Glu[19] analogue at the PTH1(delta-N-terminus) receptor (*1*). This clearly indicates that the region (residues 15−20) between the traditionally defined "binding" and "activation" domains of PTH contributes to the interaction with the juxtamembrane portion of the PTH1 receptor and that a α-helix facilitates this interaction. In other words, the Glu[19] → Arg[19] substitution seems to improve the binding mainly by stabilizing the free ligand in a helical conformation which corresponds, or is very close to, the one assumed by the peptide in the complex with the receptor. This therefore suggests that the residue in position 19 does not interact specifically with the receptor and that every amino acid preserving the helical content (e.g., Aib) could replace Arg[19] without affecting the receptor affinity. Further predictions would be risky at this point, as it is still not completely understood how the Glu[19] → Arg[19] leads to the helical content improvement observed with the CD experiments, especially in the PTH(1−34) analogues. Efforts to incorporate these recent findings into a molecular model of the PTH/PTH1 ligand/receptor complex are currently ongoing.

ACKNOWLEDGMENT

The authors thank Maria Pellegrini (Biogen) for helpful discussions and reading of the manuscript and Iris Escher of the Greg Verdine laboratory (Harvard Chemistry Department) for providing equipment for and assistance with the CD experiments.

REFERENCES

1. Shimizu, M., Shimizu, N., Tsang, J., Petroni, B. D., Khatri, A., and Gardella, T. J. (2002) *Biochemistry 41*, 13224−13233.
2. Yang, J. T., Wu, C. S., and Martinez, H. M. (1986) *Methods Enzymol. 130*, 208−69.
3. Fasman, G. D. (1996) *Circular Dichroism and the Conformational Analysis of Biomolecules*, Plenum, New York.
4. Braunschweiler, L., and Ernst, R. R. (1983) *J. Magn. Reson. 53*, 521−528.
5. Bax, A., and Davis, D. G. (1985) *J. Magn. Reson. 65*, 355−360.
6. Macura, S., Huang, Y., Suter, D., and Ernst, R. R. (1981) *J. Magn. Reson. 43*, 259−281.
7. Piotto, M., Saudek, V., and Sklenar, V. (1992) *J. Biomol. NMR 2*, 661−5.
8. Delaglio, F., Grzesiek, S., Vuister, G. W., Zhu, G., Pfeifer, J., and Bax, A. (1995) *J. Biomol. NMR 6*, 277−93.

9. Goddard, T. D., and Kneller, D. G. (2001) *SPARKY 3*, University of California, San Francisco.
10. Wishart, D. S., Sykes, B. D., and Richards, F. M. (1992) *Biochemistry 31*, 1647−1651.
11. Wuthrich, K., Billeter, M., and Braun, W. (1983) *J. Mol. Biol. 169*, 949−61.
12. Havel, T. F. (1991) *Prog. Biophys. Mol. Biol. 56*, 43−78.
13. Berendsen, H. J. C., van der Spoel, D., and van Buuren, R. (1995) *Comput. Phys. Comm. 95*, 43−56.
14. van Buuren, A. R., Marrink, S., and Berendsen, H. J. C. (1993) *J. Phys. Chem. 97*, 9206−9216.
15. Sargent, D. F., and Schwyzer, R. (1986) *Proc. Natl. Acad. Sci. U.S.A. 83*, 5774−5778.
16. Schwyzer, R. (1991) *Biopolymers 31*, 785−792.
17. Schwyzer, R. (1992) *Braz. J. Med. Biol. Res. 25*, 1077−1089.
18. Moroder, L., Romano, R., Guba, W., Mierke, D. F., Kessler, H., Delporte, C., Winand, J., and Christophe, J. (1993) *Biochemistry 32*, 13551−13559.
19. Moroder, L. (1997) *J. Pept. Sci. 3*, 1−14.
20. Inooka, H., Ohtaki, T., Kitahara, O., Ikegami, T., Endo, S., Kitada, C., Ogi, K., Onda, H., Fujino, M., and Shirakawa, M. (2001) *Nat. Struct. Biol. 8*, 161−165.
21. Shoemaker, K. R., Kim, P. S., York, E. J., Stewart, J. M., and Baldwin, R. L. (1987) *Nature 326*, 563−7.
22. Pellegrini, M., Royo, M., Rosenblatt, M., Chorev, M., and Mierke, D. F. (1998) *J. Biol. Chem. 273*, 10420−10427.
23. Neugebauer, W., Barbier, J.-R., Sung, W. L., Whitfield, J. F., and Willick, G. E. (1995) *Biochemistry 34*, 8835−8842.
24. Neugebauer, W., Surewicz, W. K., Gordon, H. L., Somorjai, R. L., Sung, W., and Willick, G. E. (1992) *Biochemistry 31*, 2056−2063.
25. Schievano, E., Mammi, S., Silvestri, L., Behar, V., Rosenblatt, M., Chorev, M., and Peggion, E. (2000) *Biopolymers 54*, 429−47.
26. Condon, S. M., Morize, I., Darnbrough, S., Burns, C. J., Miller, B. E., Uhl, J., Burke, K., Jariwala, N., Locke, K., Krolikowski, P. H., Kumar, N. V., and Labaudiniere, R. F. (2000) *J. Am. Chem. Soc. 122*, 3007−3014.
27. Marx, U. C., Adermann, K., Bayer, P., Forssmann, W. G., and Rosch, P. (2000) *Biochem. Biophys. Res. Commun. 267*, 213−20.
28. Barden, J. A., and Kemp, B. E. (1996) *Biochem. Biophys. Res. Commun. 220*, 431−436.
29. Marx, U. C., Adermann, K., Bayer, P., Meyer, M., Forssmann, W. G., and Rosch, P. (1998) *J. Biol. Chem. 273*, 4308−16.
30. Barden, J. A., and Kemp, B. E. (1993) *Biochemistry 32*, 7126−7132.
31. Chen, Z., Xu, P., Barbier, J. R., Willick, G., and Ni, F. (2000) *Biochemistry 39*, 12766−77.
32. Peggion, E., Mammi, S., Schievano, E., Behar, V., Rosenblatt, M., and Chorev, M. (1999) *Biopolymers 50*, 525−35.
33. Jin, L., Briggs, S. L., Chandrasekhar, S., Chirgadze, N. Y., Clawson, D. K., Schevitz, R. W., Smiley, D. L., Tashjian, A. H., and Zhang, F. (2000) *J. Biol. Chem. 275*, 27238−44.
34. Rolz, C., Pellegrini, M., and Mierke, D. F. (1999) *Biochemistry 38*, 6397−6405.

BI0261600